

Geology of the Bungalow Pluton, Clearwater County, Idaho

Abstract

The Bungalow granite pluton is one of several relatively unstudied Eocene age (37-52 Ma) plutons located within the Clearwater igneous province of northern Idaho. This province lies along the Kelly Forks fault, a major northwest-trending strike-slip structure that separates the Cretaceous age (60-90 Ma) Idaho batholith from Proterozoic (850-1400 Ma) metamorphic rocks. This study used geologic mapping, together with whole rock geochemical analyses and petrographic thin section observations, to document the internal chemical, petrographic and structural characteristics of the pluton and to reconstruct the crystallization behavior and mode of emplacement. The pluton forms a 225 km² by 1600 m exposure of granite with steep, unaltered and undeformed margins and a well defined negative gravity anomaly. The west half of the pluton has an upper surface of porphyritic granite. The large NW -trending Kelly Forks fault and 3 N-S striking normal faults cut the pluton. These new observations, interpreted in context of previous limited radiometric age dating and structural analysis of the Kelly Forks fault, suggest that the pluton is an isolated body passively emplaced along a strike-slip tectonic setting which was active during the Paleogene. This setting contrasts with the northeast-trending normal faults associated with Eocene igneous provinces adjacent to the southern part of the Idaho batholith. The pluton is composed of a suite of texturally diverse (fine-grained to porphyritic), yet remarkably homogeneous high-silica (75-77 wt % SiO₂), metaluminous, biotite granite. The preferential occurrence of porphyritic textures and hydrous minerals near the edges of the pluton suggest that the pluton crystallized from the margins inward with no significant differentiation. In addition, the pluton was intruded by minor occurrences of rhyolite porphyry dikes, quartz syenite, lamprophyre dikes and has subsequently undergone limited, post magmatic hydrothermal alteration.

Introduction

Ongoing geologic studies adjacent to the Cretaceous Idaho batholith located in northern and central Idaho have documented numerous Eocene intrusive and volcanic provinces (Lewis et al., 1992a, 1992b; Lewis and Kiilsgaard, 1991; Reynolds, 1991; Lewis, 1990; Motzer, 1985; Simpson, 1985; Bennett and Knowles, 1983; Hardyman, 1981; Nold, 1968; Hietanen, 1963). These provinces have been interpreted by most previous researchers to represent post-orogenic igneous activity following the subduction-related generation of the Idaho batholith. Many of these Eocene plutons have been mapped and sampled on reconnaissance scale, but little has been done to document in detail their internal petrographic and geochemical variability or to establish the structural controls on emplacement and post magmatic deformation.

This paper presents new field and geochemical information to document the internal petrologic and structural character of the Bungalow pluton, one of a series of chemically diverse Eocene intrusions and volcanic centers that make up the Clearwater igneous province of northern Idaho. The data suggest that this high-silica pluton is surprisingly homogeneous and developed by inward crystallization. The pluton has also been

intruded by later dikes and undergone late stage hydrothermal alteration resulting in mineral assemblages and geochemical anomalies not observed in other Eocene plutons surrounding the Idaho batholith. Structural observations indicate that igneous activity associated with the Clearwater igneous province, and the Bungalow pluton in particular, is closely confined to a northwest-trending strike-slip fault system that was active during the Paleogene (Ewing, 1980). This tectonic setting is in contrast to northeast-trending extensional faults associated with Eocene igneous provinces adjacent to the Atlanta lobe of the Idaho batholith (Bennett, 1986; Motzer, 1985).

Field Relations

Geologic Setting

The Bungalow pluton intrudes the northern margin of the Bitterroot lobe of the Idaho batholith and Proterozoic metasediments of the Belt Supergroup (Fig. 1). It is dissected by the North Fork of the Clearwater River, providing 1600 m of vertical exposure. The pluton lies adjacent to and is partly cut by the Kelly Forks fault, one of several large northwest trending fault zones that transect northern Idaho. The fault forms a km-wide zone of deformation that separates the older

Clearwater Igneous Province

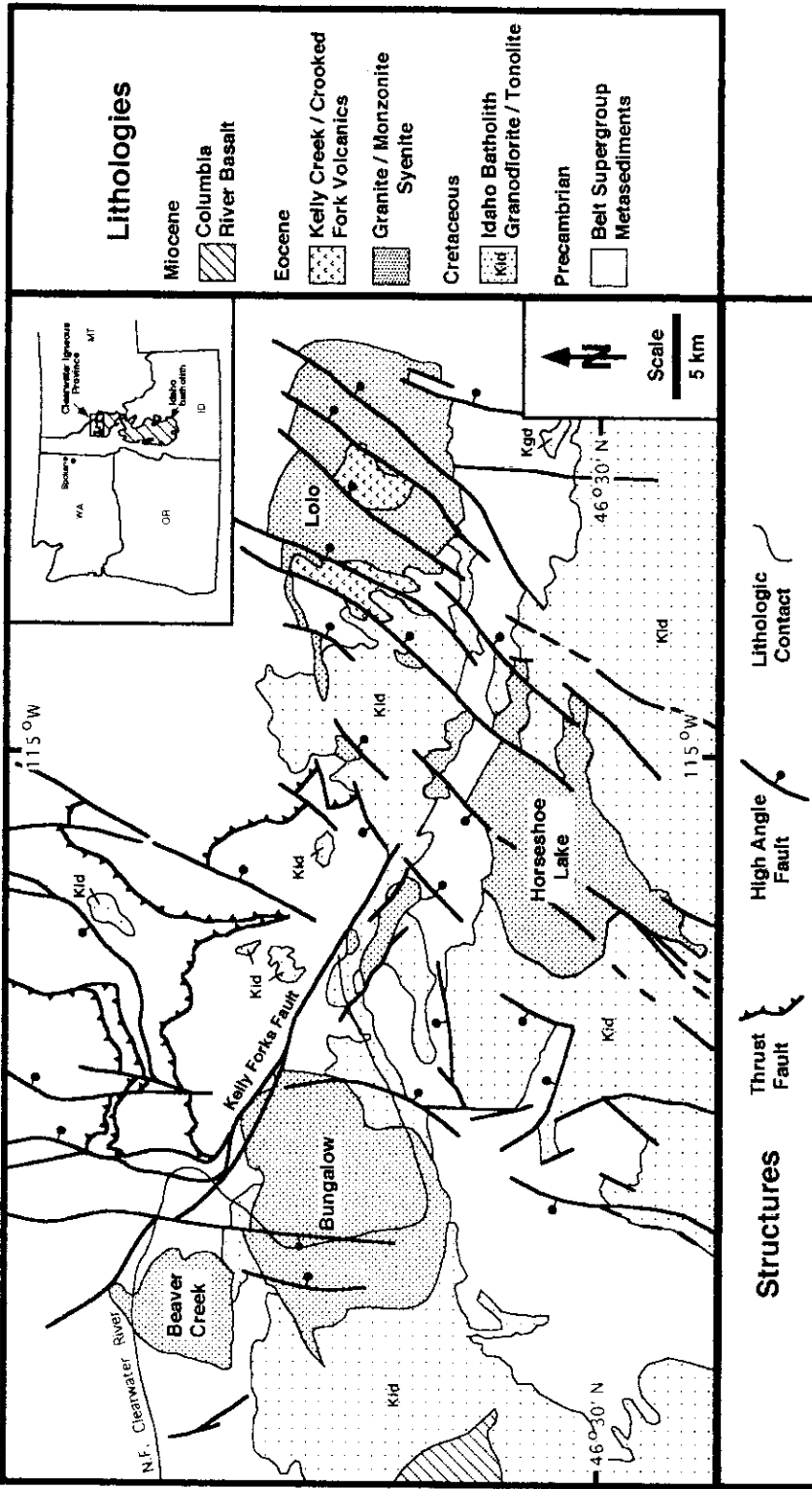


Figure 1. Simplified geologic map of the Clearwater igneous province highlighting Eocene intrusions and major structural features (compiled from Lewis et al., 1992a, 1992b; Reynolds, 1991; Bennett, 1986).

igneous and metamorphic country rocks. An array of Eocene plutons that compose the Clearwater igneous province have intruded along the fault zone (Fig. 1). Childs (1983) has provided evidence that alternating episodes of kilometer-scale right- and left-lateral strike-slip movement have occurred along the fault during the Paleogene. However, offset of the Bungalow pluton by the Kelly Forks fault is minimal, with latest movement consisting of right-lateral oblique-slip movement. North of the Kelly Forks fault, Belt Supergroup metasediments are complexly folded and thrust faulted. South of the fault, large expanses of Cretaceous tonalite and granodiorite, together with lesser amounts of Precambrian metamorphic rock, are exposed. A series of steep-dipping, northeast-trending faults cut the plutonic rocks and truncate the southeast end of the Kelly Forks fault. Other Eocene plutons located within the Clearwater igneous province and along the northwest trend of the Kelly Forks fault include the Beaver Creek stock, the Horseshoe Lake pluton, the Lolo Hot Springs pluton, and numerous unnamed bodies of syenite (Fig. 1; Lewis et al., 1992a). Rhyolite dikes are generally abundant throughout the Clearwater igneous province and intrude all the plutons (Lewis et al., 1992a).

Potassium/argon age determinations on biotite, 45 +/- 2.0 Ma. (Armstrong, et al., 1977) and 43.1 +/- 1.4 Ma (Hietanen, 1969), provide the only available age constraints for the Bungalow pluton. Owing to the overall medium to coarse-grained texture of the pluton, which suggests slow cooling and extensive subsolidus recrystallization, the ages could be anomalously young, reflecting cooling ages rather than crystallization ages. Clearly, age determinations of fine-grained granite and crosscutting dikes are needed. Nevertheless, the available age data contrast with the late Cretaceous ages (65-90 Ma) assigned to plutons of the Bitterroot lobe of the Idaho batholith and are remarkably similar to numerous other Eocene plutons in the region which span an age range of 38-50 Ma (Armstrong, 1974).

Form of Intrusion

The Bungalow pluton forms a continuously exposed body approximately 15 km in diameter and 1600 m thick (Fig. 2). The floor is not exposed. Contacts between the pluton and country rock are steep-dipping and abrupt. No evidence of xeno-

liths or flow foliation occur in the granite nor has there been any appreciable contact metamorphism or hydrothermal alteration of the adjacent country rock. This is in contrast to other more mafic Eocene plutons adjacent to the Idaho batholith, such as the Beaver Creek stock, which show well defined igneous foliation and abundant xenoliths.

Reconnaissance gravity survey data indicate the existence of a large, well-defined negative gravity anomaly centered over the pluton and supports field observations that the pluton is steep-sided and upright (Zeitz et al., 1978). Moreover, the negative gravity anomaly, together with the absence of a distinct magnetic anomaly, suggest that the pluton has no mafic root; the pluton is therefore an isolated igneous body.

The west half of the pluton is topographically subdued. Irregular sheets of porphyritic granite are exposed over much of this area. Porphyritic granite is partly surrounded by fine-grained granite and grades downward into medium- and coarse-grained granite. Vertical exposures of porphyritic granite range from 100 to 400 m.

Rhyolite porphyry dikes intrude the margins and interior of the pluton and surrounding country rock in numerous locations (Fig. 2). The dikes form narrow, resistant, steeply dipping ridges that can be traced for hundreds of meters to over 12 km, and range in width from 3 to 30 m. In addition, a northeast-trending swarm of rhyolite dikes occurs near the southeastern margin of the pluton (Fig. 2; Lewis et al., 1992a).

A few lamprophyre dikes are exposed within and around the pluton. They occur as dark, solitary, near-vertical dikes 1 to 3 m wide exposed for hundreds of meters along strike. At some contacts, the adjacent granite has been baked and altered, indicating that the dikes were emplaced at high temperature into solidified granite. In no cases are the dikes observed to be in a state of disaggregation or partial assimilation. The occurrence of crosscutting, undeformed lamprophyre dikes, the first to be documented in the Eocene plutons surrounding the Idaho batholith, provides a significant contrast to the older (Cretaceous), deformed and comingled, synplutonic, mafic dikes within the plutons of the Idaho batholith (Hyndman and Foster, 1988).

A small (1 km²) pod of altered quartz syenite is located within the porphyritic granite section of the Bungalow pluton. Its vertical exposure is

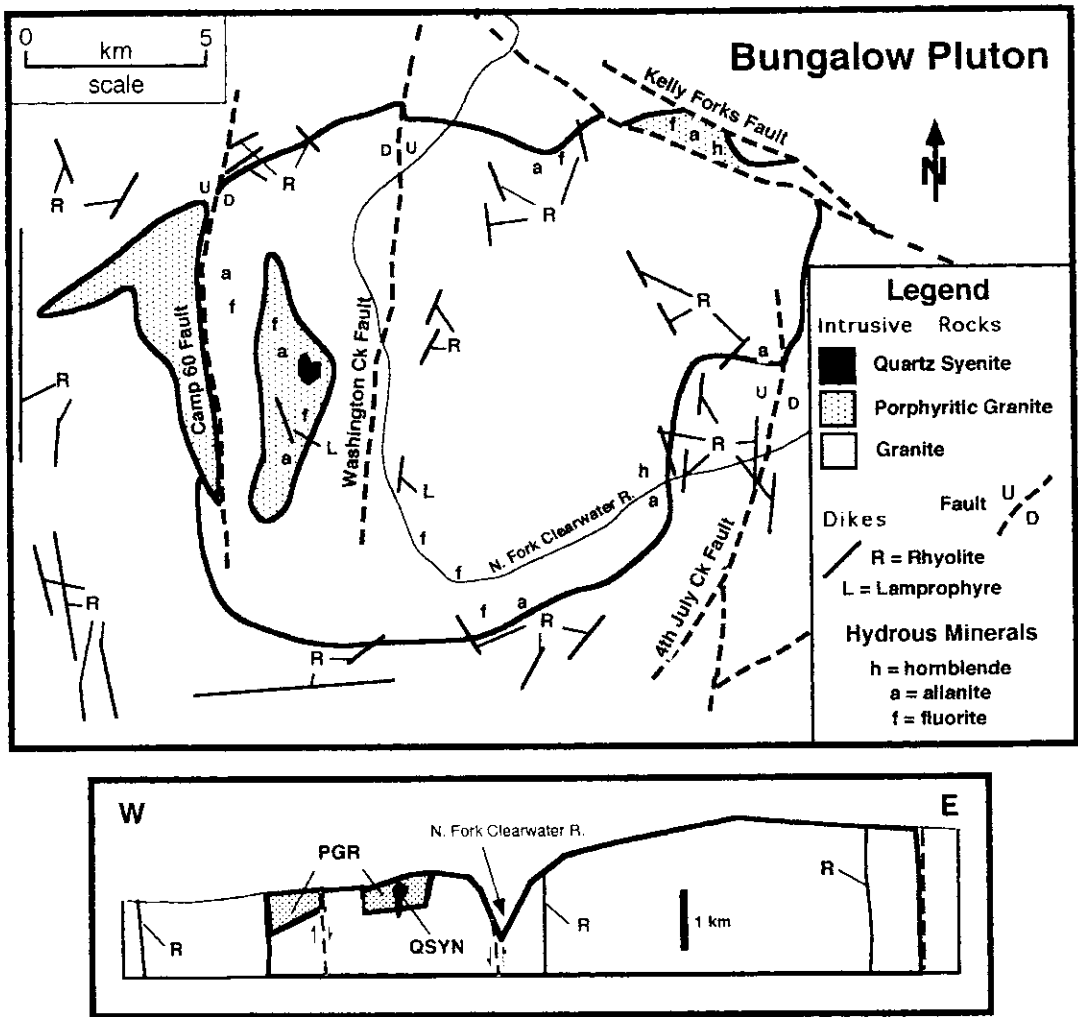


Figure 2. Geologic map and interpretative W-E cross section of the Bungalow pluton showing major rock types, cross cutting faults and dikes and the distribution of hydrous minerals compiled from Lewis et al., 1992a; Reynolds, 1991; Hietanen, 1963).

200 m. A 3 m wide fine-grained margin marks the northern contact with porphyritic granite, whereas the interior is coarse grained. An abundance of fractured mineral grains and cloudy feldspar indicate that hydrothermal alteration was focused on the quartz syenite. More extensive outcrops of syenite have been mapped in the region outside of the complex as separate intrusions (Fig. 1; Lewis et al., 1992a).

Greisenized granite forms groups of vertical veins and subhorizontal lenses in the southwest-ern quarter of the pluton. Veins and lenses vary

in size from 0.5 to 2 m thick by 1 to 5 m long and are sharply discordant with the wall rock. The veins show no preferred orientation and appear to have developed independently of the well-developed north-trending joint pattern in the granite.

The pluton is deformed by three north-trending high angle normal faults. Evidence for these faults is abundant in the northern part of the pluton, but becomes more obscure to the south perhaps indicative of greater fault displacement to the north. The most prominent fault is the Washington Creek fault that splits the pluton roughly

in half (Fig. 2). The west half of the pluton is the down thrown block with a possible displacement of 100 to 700 m. Two other faults bound the east and west margins of the pluton. The western-most fault, exposed at Camp 60, together with the Washington creek fault, separate a down-dropped block of porphyritic granite from an uplifted eastern block of coarse-grained granite. On the extreme east side of the pluton a large north-trending fault is well exposed at Fourth of July creek. This fault offsets Cretaceous igneous rocks, as well as rhyolite dikes with the east block down-dropped. All of the north and northeast-trending faults in the region postdate the Kelly Forks fault, yet predate the extrusion of Columbia River basalt (Lewis et al., 1992a).

Petrography

The granitoid rocks within the pluton are divided by grain size and texture. Thin section point counts of 1000 points per sample were used to derive the normalized modal mineral distribution for the three major phases (Table 1 and Fig. 3) and to determine the type and amount of accessory minerals present. The bulk of the pluton is composed of light-gray, fine-, medium- and coarse-grained, subsolvus biotite granite. Representative samples are hypidiomorphic equigranular and contain subequal proportions of perthitic orthoclase, plagioclase and quartz. The dominant mafic mineral is brown biotite which occurs throughout the pluton in modal amounts of 1-5%. Trace amounts of allanite, apatite, zircon and magnetite are also present. Rare occurrences of fluorite and extensively-replaced hornblende are found near the margins of the pluton, whereas biotite is distributed equally throughout the pluton. Porphyritic granite occurs over large parts of the western half of the pluton and is composed of large euhedral phenocrysts of orthoclase and quartz set in a fine-grained to granophyric groundmass.

Rhyolite dikes consist of a blue-gray groundmass in which euhedral pink orthoclase, white plagioclase, and bipyramidal smoky quartz phenocrysts are embedded. Phenocryst contents range from 17-51 modal %. Accessory biotite is present along with trace amounts of pyroxene, amphibole, apatite, zircon, magnetite, and fluorite. Millimeter-scale flow-banding is present in some rhyolite dikes. Banding occurs as dark-gray layers of obsidian and quartz-feldspar spherulites that

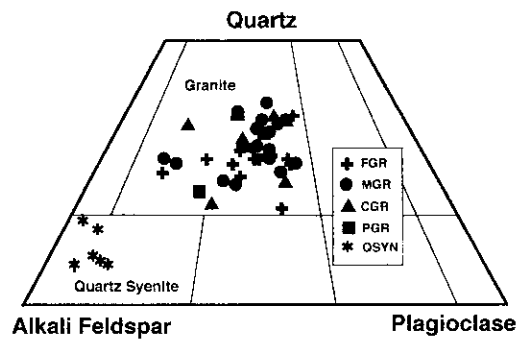


Figure 3. Modal distribution of plutonic rocks associated with the Bungalow pluton. Modes were determined by petrographic thin section point counting (see also Table 1). Symbols: FGR = fine-grained granite, MGR = medium-grained granite, CGR = coarse-grained granite, PGR = porphyritic granite, QSYN = quartz syenite.

are separated by a pale white, fine-grained matrix of plagioclase, K-feldspar and quartz. Banding roughly parallels the walls of the dikes and is commonly convoluted.

Yellow-brown to dark-gray lamprophyre dikes consist of a sparsely porphyritic, intergranular arrangement of battlemented biotite laths (26-49 modal %), together with subequal amounts of plagioclase, potassium feldspar, and augite. Large (1-3 cm) isolated crystals of pink orthoclase are the only visible phenocrysts. Small (1-3 mm) vug-like cavities lined with quartz and calcite are abundant in some of the lamprophyres.

The mineralogy of the quartz syenite includes milky-white perthitic alkali feldspar, albite, and dark green clots of aegirine-augite. Much of the alkali feldspar exhibits a checkerboard pattern, indicative of pervasive albitic alteration (Parsons and Brown, 1984). The larger plagioclase phenocrysts are strained and cracked from post-crystallization deformation. In addition, a very-fine-grained acicular blue amphibole, possibly arfvedsonite or riebeckite, partly replaces pyroxene. Accessory minerals include siderite and specular hematite. Fluorite and topaz are present in trace amounts. Although small in size, the sodium-rich quartz syenite is the first to be described from Eocene granites adjacent to the Idaho batholith. Other Eocene syenites described thus far from the Clearwater igneous province are not hydrothermally altered.

TABLE 1. Normalized modal point counts of 46 granite thin sections vs elevation and distance from pluton margin

Sample	Elevation	Distance	Texture	Quartz	K-spar	Plag	Biotite	h	f	a	ap	mia
203	1591	0.1	APL	34	31	35	G					
35	1070	1.4	APL	43	33	23	G4		X	X	X	
120	1246	4.6	APL	22	35	43	BG2					
368	914	0.7	APL	30	31	39	B7		X	X	X	
67	1366	0.3	FGR	33	35	32	GM3			X		
193	2048	2.8	FGR	33	28	39	BMG					F
192	2060	2.8	FGR	34	32	34	B6					F
364	1905	2.4	FGR	27	42	31	BG3					
340	1768	1.2	FGR	41	26	33	B6		X			
462	786	0.1	FGR	39	30	31	G3					
289	1524	0.8	FGR	35	31	34	BMG5				X	
259	1271	4.3	FGR	42	24	34	G1					
14	780	0.1	FGR	43	26	31	BM3					
301	1524	0.4	FGR	28	44	72	G2		X			F
355	649	6.5	FGR	39	30	31	BG3					F
327	1753	2.7	MGR	39	29	32	BM4					
27	646	4.0	MGR	38	35	27	BG4					A
34	671	4.5	MGR	36	35	29	G2		X			
59	671	4.8	MGR	42	24	34	BMG4		X			
105	1341	2.7	MGR	39	30	31	B4					
329	1737	2.2	MGR	33	32	35	BMG4					
22	702	1.2	MGR	28	31	41	BMG4		X			F
291	1561	0.2	MGR	33	34	33	B6	1		X	X	
175	646	4.5	MGR	32	28	40	B5			X	X	
243	786	0.1	MGR	35	37	28	B5			X	X	
302	1524	0.7	MGR	32	52	16	G3	1	X	X	X	A
305	1412	1.1	MGR	32	27	41	G6					F
363	1981	1.9	MGR	40	31	29	BM3					
258	1545	6.5	MGR	33	32	35	GM4		X			
244	738	1.0	MGR	36	36	28	B3		X			
245	732	1.5	MGR	36	36	28	BM3					
90	1158	3.4	MGR	29	40	31	B5		X	X	X	
261	1049	3.4	MGR	36	33	31	B5		X			
13	1073	0.8	CGR	23	49	28	B7					
4	610	0.5	CGR	44	33	23	B6		X	X	X	
10	1091	2.7	CGR	41	45	14	B7			X	X	
283	704	1.0	CGR	46	26	28	B6			X		
184	1597	0.6	CGR	30	56	14	GM6	X		X		A
403	610	1.4	CGR	44	33	23	B5		X	X		
296	1524	0.8	CGR	33	54	13	BG3		X	X		
81	1052	2.0	CGR	32	40	28	B4		X	X	X	
456	631	3.2	CGR	26	50	24	B3					
109	1329	3.5	PGR	33	45	22	B5			X		A
110	1311	3.4	PGR	43	22	35	B10		X	X	X	
373	1146	7.5	PGR	42	29	29	B5		X	X		

key to headings and symbols for hydrous minerals:

Biotite: B = brown biotite; G = green biotite; M = muscovite; numbers = modal percent
h = hornblende, numbers = modal percent; f = fluorite, a = allanite, ap = apatite,
x = presence in sample; mia = occurrence of miarolitic cavities, F = few, A = abundant

The greisens within the pluton consist of a vein-controlled hydrothermal alteration mineral assemblage dominated by quartz (60-80 modal %) and muscovite (20-40 modal %) with accessory cassiterite and specular hematite and trace fluorite and topaz. Quartz has recrystallized into small anhedral grains that exhibit undulatory extinction and sutured grain boundaries. Muscovite has replaced nearly all of the feldspar and biotite. Cassiterite is disseminated throughout the greisens as 0.05-0.3 mm euhedral hexagons, whereas topaz forms isolated, octagonal grains rimmed by muscovite.

Geochemistry

Thirty eight representative samples of the pluton were analyzed, including granite (22 samples), rhyolite, quartz syenite and hydrothermally altered rocks. Two blind duplicates were analyzed with each set of samples. Chemex Laboratory Inc. performed the whole-rock determinations of 11 major element oxides. 1-2 kg hand samples were submitted to multiple stage crushing and pulverizing to -150 mesh in a zirconia ring. After pulverizing, 20 gram sub-samples were selected, fused and then analyzed by inductively coupled plasma-atomic emission spectroscopy (ICP-AES). Detection limits were 0.01 wt % for each oxide. Ferrous iron content was determined separately by acid decomposition-titration. Major element oxides were reproducible to less than 5 wt % (except TiO_2 and P_2O_5). Bondar-Clegg Inc. performed the minor and trace element analyses on each of the granites. These samples were prepared in a manner similar to the whole-rock sample preparation methods and analyses were obtained by instrumental neutron activation analysis (INAA). Trace elements were reproducible to less than 15 % (except Yb). The analytical results, together with standard deviations and duplicate analyses are compiled in Table 2.

Major Elements

The major element oxide abundances for the granite are remarkably homogeneous (Table 2). The granites are high-silica (75-77 wt %) and metaluminous to weakly peraluminous (Fig. 4). MgO and CaO show a reciprocal relationship as SiO_2 increases (Fig. 5). Trends for K_2O and Na_2O are poorly developed and may be affected by deuteric alteration. The major element composi-

tions of the rhyolite porphyry dikes are very similar to the granite (Table 2). The hydrothermal alteration has affected some of the apical parts of the pluton and masks some of the chemical characteristics of the granitic rocks. For example, the quartz syenite is complicated by an overprint of sodium enrichment indicative of albitic alteration (Table 2).

Trace Elements

Compositional variations for most of the trace elements in granite are not significant (Table 2 and Fig. 5). Barium however, decreases with increasing silica, and chondrite-normalized rare earth elements (REE) decrease with increasing atomic number (Fig. 6). All granites show a pronounced negative Eu anomaly, with porphyritic granite having the smallest Eu anomaly. The albitized quartz syenite is enriched in Ba and light REE and depleted in Rb and heavy REE relative to granite (Table 2). Greisens contain elevated amounts of Cs, Rb, Th and U (Table 2) as well as anomalous Sn, Mo, W, Nb, and Ag values (Reynolds, 1991).

Volatiles

Little information is available to help constrain the volatile content of the magma. The only hydrous mineral present in accessory amounts is biotite (Table 1). Rare hornblende (extensively replaced by biotite) and trace amounts of apatite and topaz are present and concentrated in the marginal regions of the pluton (Table 1, Fig. 2) where water was presumed to be more abundant. In addition, the chlorine content of biotite is highest in samples taken from porphyritic granite near the projected roof of the pluton (Reynolds, 1991). Small (0.5-1 cm) miarolitic cavities are observed in 26 % of the hand specimens and thin sections (Table 1). The miarolitic cavities are abundant throughout the pluton and become larger with increasing elevation and towards the margins of the pluton. The cavities provide evidence that water exsolved in the late stages of crystallization.

Discussion

Emplacement

The emplacement and subsequent deformation of the Bungalow pluton appear to have been controlled primarily by the Kelly Forks fault and a

TABLE 2. Major and trace element whole rock analyses for the Bungalow pluton and associated rocks.

	FGR		(n=6)		MGR		(n=10)		CGR		(n=4)		PGR		(n=2)		QSYN		(n=4)		GREI		(n=2)	
	Avg	Stdev	Avg	Stdev	Avg	Stdev	Avg	Stdev	Avg	Stdev	Avg	Stdev	Avg	Stdev	Avg	Stdev	Avg	Stdev	Avg	Stdev	Avg	Stdev	Avg	Stdev
SiO ₂	76.88	0.41	77.02	0.90	76.13	0.64	74.89	0.49	76.54	0.92	56.21	0.66	70.22	0.06	78.43	4.16								
TiO ₂	0.04	0.02	0.06	0.04	0.12	0.05	0.20	0.08	0.15	0.06	1.61	0.23	0.20	1.03	0.06	0.01								
Al ₂ O ₃	12.85	0.28	12.59	0.37	12.79	0.23	13.36	0.07	12.70	0.45	16.50	0.24	15.38	1.05	12.62	2.48								
HFO	0.81	0.16	0.86	0.14	1.01	0.09	1.40	0.33	0.78	0.34	5.24	1.70	1.18	0.75	2.43	0.25								
Fe ₂ O ₃	0.16	0.08	0.25	0.16	0.44	0.13	0.24	0.15	0.63	0.28	2.29	1.61	1.14	0.01	1.76	0.84								
MnO	0.03	0.02	0.03	0.01	0.02	0.01	0.03	0.01	0.02	0.01	0.13	0.02	0.03	0.10	0.12	0.12								
MGO	0.35	0.22	0.07	0.04	0.18	0.09	0.29	0.03	0.11	0.07	3.04	0.05	0.28	0.23	0.11	0.06								
CaO	0.06	0.03	0.52	0.32	0.77	0.53	1.09	0.08	0.65	0.23	5.52	0.21	1.02	2.22	0.20	0.08								
Na ₂ O	4.14	0.31	3.97	0.35	3.66	0.21	3.58	0.01	3.70	0.31	5.21	0.15	7.11	1.94	0.21	0.01								
K ₂ O	4.60	0.37	4.47	0.57	4.85	0.26	4.87	0.01	4.70	0.27	3.84	0.95	3.40	0.03	4.01	0.85								
P ₂ O ₅	0.07	0.06	0.06	0.04	0.06	0.04	0.08	0.06	0.05	0.04	0.48	0.06	0.04	0.04	0.02	0.01								

Trace Elements (ppm)	Cs		Rb		Th		U		Ta		Ba		Hf		La		Ce		Sm		Eu		Tb		Yb		Lu				
	Avg	Stdev	Avg	Stdev	Avg	Stdev	Avg	Stdev	Avg	Stdev	Avg	Stdev	Avg	Stdev	Avg	Stdev	Avg	Stdev	Avg	Stdev	Avg	Stdev	Avg	Stdev	Avg	Stdev	Avg	Stdev			
Cs	6	4	7	2	4	3	4	1	3	1	1	1	1	1	1	1	1	1	1	1	1	1	1	1	1	1	1	1	1		
Rb	349	180	216	33	164	47	160	85	209	64	124	56	616	50	192	8	14	14	14	14	14	14	14	14	14	14	14	14	14	14	
Th	24.1	2.8	20.4	5.2	17.4	3.7	17.4	7.6	20.7	4.9	23.1	0.6	34.9	1.7	13.1	7.3	7.3	7.3	7.3	7.3	7.3	7.3	7.3	7.3	7.3	7.3	7.3	7.3	7.3	7.3	
U	6.8	2.7	5.2	1.7	4.2	1.5	4.2	1.3	5.3	2.0	3.9	1.0	9.2	1.1	3.7	1.7	1.7	1.7	1.7	1.7	1.7	1.7	1.7	1.7	1.7	1.7	1.7	1.7	1.7	1.7	
Ta	5.1	4.7	2.2	1.0	1.1	0.7	1.0	0.6	1.6	0.8	1.4	0.4	4.4	1.6	1.2	0.5	0.5	0.5	0.5	0.5	0.5	0.5	0.5	0.5	0.5	0.5	0.5	0.5	0.5	0.5	
Ba	42	12	74	41	180	67	340	14	143	175	698	198	25	0	450	551	551	551	551	551	551	551	551	551	551	551	551	551	551	551	
Hf	6	2	4	1	5	2	5	1	5	2	6	1	3	1	4	2	2	2	2	2	2	2	2	2	2	2	2	2	2	2	
La	12	5	21	13	43	8	43	23	34	17	63	27	13	1	29	13	13	13	13	13	13	13	13	13	13	13	13	13	13	13	
Ce	25	8	35	19	71	11	69	15	65	27	108	18	27	3	51	19	19	19	19	19	19	19	19	19	19	19	19	19	19	19	19
Sm	3.7	1.5	4.5	1.4	6.0	1.0	5.8	1.4	6.6	1.9	10.4	2.1	6.0	0.2	5.8	2.2	2.2	2.2	2.2	2.2	2.2	2.2	2.2	2.2	2.2	2.2	2.2	2.2	2.2	2.2	
Eu	0.2	0.2	0.2	0.1	0.3	0.2	0.5	0.0	0.4	0.2	0.5	0.0	0.5	0.0	0.3	0.2	0.2	0.2	0.2	0.2	0.2	0.2	0.2	0.2	0.2	0.2	0.2	0.2	0.2	0.2	0.2
Tb	0.9	0.5	1.2	0.3	0.9	0.5	0.7	0.5	1.4	0.3	1.3	0.2	1.7	0.4	1.1	0.4	0.4	0.4	0.4	0.4	0.4	0.4	0.4	0.4	0.4	0.4	0.4	0.4	0.4	0.4	0.4
Yb	4.16	1.84	5.08	1.89	2.76	1.97	1.95	0.08	3.80	1.59	2.25	0.50	3.50	0.71	3.11	1.49	1.49	1.49	1.49	1.49	1.49	1.49	1.49	1.49	1.49	1.49	1.49	1.49	1.49	1.49	1.49
Lu	0.65	0.34	0.88	0.29	0.47	0.33	0.38	0.04	0.67	0.20	0.45	0.06	0.65	0.07	0.50	0.23	0.23	0.23	0.23	0.23	0.23	0.23	0.23	0.23	0.23	0.23	0.23	0.23	0.23	0.23	0.23

*whole rock values are normalized to 100% water free n = sample population

Rock Type abbreviations:

FGR = fine-grained granite; MGR = medium-grained granite; CGR = coarse-grained granite; PGR = porphyritic granite

LAM = lamprophyre dikes; QSYN = quartz syenite; GREI = gresien

TABLE 2. (Con't)

Duplicate analyses (normalized to 100 % water free)						
Sample #	30	30-D	% Dif	455	455-D	% Dif
SiO ₂	74.59	74.61	0.0	76.18	76.44	0.3
TiO ₂	0.23	0.20	14.0	0.02	0.02	0.1
Al ₂ O ₃	13.69	13.62	0.5	13.21	13.02	1.5
FeO	1.46	1.53	4.7	0.56	0.55	1.8
Fe ₂ O ₃	0.56	0.52	7.6	0.23	0.23	0.1
MnO	0.03	0.03	0.1	0.05	0.05	0.1
MGO	0.03	0.03	0.1	0.07	0.07	0.1
CAO	0.66	0.63	4.8	0.46	0.48	4.4
Na ₂ O	3.99	4.02	0.9	4.38	4.33	1.1
K ₂ O	4.71	4.78	1.4	4.83	4.79	0.8
P ₂ O ₅	0.04	0.02	66.7	0.01	0.01	0.1

Bondar-Clegg standards									
Sample #	30	30-D	% Dif	455	455-D	% Dif	GS89-2	GS89-2D	% Dif
Cs	3	3	0.0	47	47	0.0	0.8	0.8	0.0
Rb	190	190	0.0	583	573	1.7	40	46	14.0
Th	18.0	20.0	10.5	27.7	27.8	0.4	3.5	3.1	12.1
U	4.5	4.9	8.5	7.8	7.9	1.3	1.4	1.4	0.0
Ta	1.2	1.4	12.5	8.5	8.4	1.2	0.30	0.30	0.0
Ba	510	560	9.3	25	25	0.0	510	540	5.7
Hf	7	8	9.2	5	6	18.2	3	3	0.0
La	53	59	10.7	9	10	10.5	10	10	0.0
Ce	110	125	12.8	17	20	16.2	24	23	4.3
Sm	8.1	8.4	3.6	5.8	5.6	3.5	1.0	1.0	0.0
Eu	0.5	0.5	0.0	0.5	0.5	0.0	0.5	0.5	0.0
Tb	1.1	1.2	8.7	1.4	1.4	0.0	0.9	0.8	11.8
Yb	1.5	3.0	66.7	4.0	4.0	0.0	3.0	3.0	0.0
Lu	0.5	0.5	0.0	0.6	0.8	28.6	0.5	0.5	0.0

Major element oxide analyses by Chemex Laboratory using ICP-AES: order #1-9024034, I9013506

Trace element analyses by Bondar-Clegg using INAA: order # R90-10599, R90-12499

% Dif = percent difference: A "D" at the end of a sample number indicates duplicate analysis

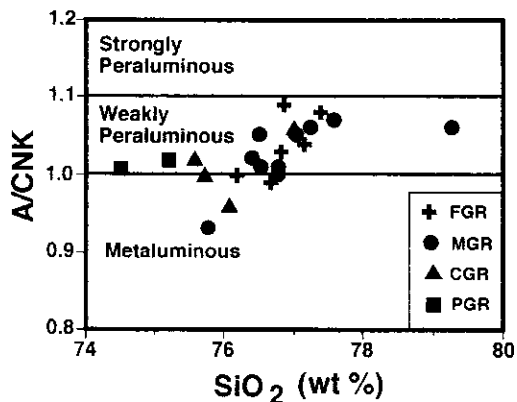


Figure 4. Plot of molecular $Al_2O_3 / CaO + Na_2O + K_2O$ (A/CNK) vs. SiO_2 for granites of the Bungalow pluton. Samples straddle the alumina saturation divide (A/CNK = 1.0) and show a subtle trend towards an increasing peraluminous character with increasing silica content. Symbol abbreviations are the same as in Fig. 3. Divisions in alumina saturation are from Ragland (1989).

few north-trending normal faults. Activation of N-W trending strike slip faults, concomitant with clockwise rotation, has been documented to have occurred in the Pacific Northwest during the Paleogene (Ewing, 1980). The Kelly Forks fault in particular is a local expression of this northwest-trending regional structure (Childs, 1983). This tectonic setting could have created NE-SW shear-induced extensional stress which facilitated emplacement. This type of extension contrasts with the NW-SE tensional basin and range type of extension found in the Challis (Bennett, 1986) and Selway-Bitterroot (Motzer, 1985) areas of central Idaho.

Reconnaissance geophysical evidence (Zeitz et al., 1978) suggests that the pluton lacks a large mafic root; it is therefore likely to be an isolated body and not the cupola of a large batholith. The lack of interaction with country rock and narrow fault margins suggest that magma ascended by

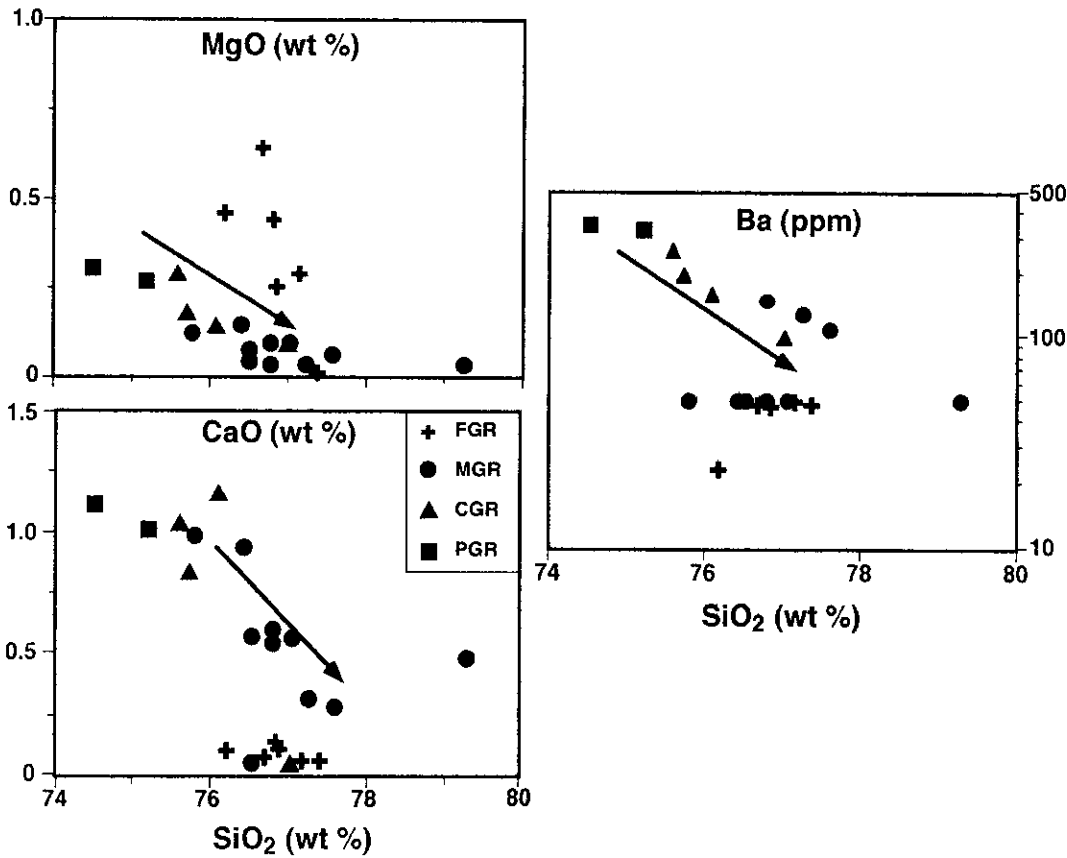


Figure 5. Representative silica covariation diagrams for the Bungalow pluton. Arrows indicate interpreted trends in selected oxides/elements versus silica. Plotted data are normalized to 100% water free. Symbol abbreviations are the same as in Fig. 3.

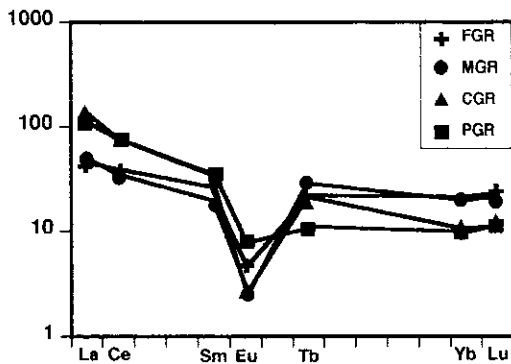


Figure 6. Chondrite normalized REE plots for the Bungalow pluton. Values shown are averages for each rock type. All rock types show a pronounced negative Eu anomaly. REE elements that were not analyzed are interpolated between the nearest analyzed neighbor elements. Symbol abbreviations are the same as in Fig. 3.

shouldering aside country rock along weak zones, rather than by forceful stopping or assimilation of the country rock. The abundance of porphyritic granite, hydrous minerals, miarolitic cavities and rhyolite porphyry dikes in the down-dropped west half of the pluton suggests that this area was close to the original roof of the pluton. Similar down-dropped blocks of foundered porphyritic roof are observed in the Challis igneous province of central Idaho (Hardyman, 1981) and in the nearby Lolo Hot Springs pluton (Fig. 1 and Nold, 1968).

Crystallization

The pluton is remarkably homogeneous in its granitic composition and appears to have crystallized from the margins of the intrusion inward. The spatial position of trace hydrous phases as well as fine-grained and porphyritic granitic

textures decrease systematically inward towards the center of the pluton, suggesting that water contents and thermal contrast were larger near the margin of the pluton. In addition, the elevated position of the porphyritic granite within the pluton suggests that it was the first to solidify as the pluton cooled.

Minor and trace element patterns provide some evidence of the crystallization pattern within the pluton. Barium, for example, decreases with increasing SiO_2 and reflects its selective incorporation into biotite and K-feldspar (Fig. 5). The pronounced light REE depletion (Fig. 6) can be attributed to the late crystallization of allanite and the negative Eu anomaly suggests that the magma was derived from a plagioclase-bearing source.

The quartz syenite bears some geochemical and spatial similarities with the porphyritic granite, but is complicated by an overprint of albitic alteration. The fine-grained margin of the quartz syenite suggests that it was emplaced after the granite had solidified, rather than developing comagmatically with the porphyritic granite. Alternatively, the margin may represent a fine-grained facies of pervasive albitic alteration resulting from second boiling of volatiles. Supporting field and petrographic evidence for this is manifest in the pervasive albitic replacement of K-feldspar and abundant fracturing of quartz and plagioclase.

The development of the quartz-muscovite greisens is also related to the concentration of magmatic fluids late in the crystallization history of the pluton. Excess magmatic pressures which can develop as a result of a vapor phase volume increase during late stage magma crystallization may have cracked the carapace of the intrusion in several places. The resulting cracks may have been invaded by acidic fluids resulting in alteration of the feldspars and biotite to produce muscovite and quartz. In addition, some of the metals (Sn, W in particular) accompanied the rising fluids.

The geochemical signature of the rhyolite porphyry dikes is very similar to the granite (Table 2). Moreover, the field occurrence of rhyolite dikes closely coincides with the margins of the pluton (Fig. 2). Because the dikes do not intrude nearby Columbia River basalt and the dikes are not commonly located in areas far from the occurrence of Eocene intrusions, the rhyolite dikes are broadly constrained in age to between middle Miocene

(17 Ma) and late Cretaceous (66 Ma). Elsewhere, surrounding the batholith, rhyolite dikes occur in similar spatial and chemical relationship with Eocene granites (Lewis et al., 1992a; Bennett, 1986; Motzer, 1985; Leonard and Marvin, 1982). Several of these rhyolite dikes have been dated and all coincide closely (± 2 my) with the time span of Eocene igneous activity in the respective areas (Marvin et al., 1989; Armstrong, 1975). Although a close spatial coincidence and chemical similarity exist between the pluton and the dikes, confirmation of a comagmatic and coeval relationship will require radiometric dating of the dikes.

Summary

The Bungalow granite pluton is important because it is one of several relatively unstudied Eocene plutons located within the Clearwater igneous province of northern Idaho that intruded along the Kelly Forks fault, a major northwest-trending strike slip structure. The pluton is a remarkably homogeneous body of texturally diverse, high-silica, biotite granite. The variation in the geochemistry of the pluton is minimal for most major and trace elements over 1.6 km of vertical relief and 225 km² of horizontal exposure. The occurrence of porphyritic textures and hydrous minerals near the margins of the pluton suggest that magma may have crystallized inward. Later subordinate rhyolite porphyry and lamprophyre dikes and a pod of quartz syenite intrude the granite. Minor post-magmatic hydrothermal alteration is confined to the upper part of the pluton and is preserved as albitic and greisenized mineral assemblages.

The pluton is a fault-bounded, steep-sided body with unaltered margins and a well defined negative gravity anomaly. The west half of the pluton has an upper surface of porphyritic granite that may represent the roof of the pluton preserved, in part, due to down dropping along N-S normal faults that post date the intrusion. These observations, when considered in context of other radiometric and structural data, suggest that the pluton is an isolated body passively emplaced in a tectonic setting which produced tensional shearing along the Kelly Forks fault as a result of strike-slip movement and clockwise rotation during the Paleogene. This tectonic setting contrasts with the northeast-trending normal faults associated with Eocene igneous provinces adjacent to the southern part of the Idaho batholith.

Acknowledgements

The author wishes to thank R. Conrey and an anonymous reviewer for the constructive comments which helped to improve the manuscript.

Literature Cited

- Armstrong, R. L. 1974. Geochrometry of the Eocene volcanic-plutonic episode in Idaho: Northwest Geology, v. 3, p. 1-15.
- . 1975. The geochronology of Idaho: Isochron/West, no. 14, p. 1-48.
- Armstrong, R. L., W. H. Taubeneck, and P. O. Hales. 1977. Rb-Sr and K-Ar geochronometry of Mesozoic granitic rocks and their Sr isotopic composition, Oregon, Washington, and Idaho: Geological Society of America Bulletin, v. 88, p. 379-411.
- Bennett, E. H. 1986. Relationship of the trans-Challis fault system in central Idaho to Eocene basin and range extensions: Geology, v. 14, p. 481-484.
- Bennett, E. H., and C. R. Knowles. 1983. Tertiary plutons and related rocks in central Idaho, *in* McIntyre, D. H., ed., Symposium on the Geology and Mineral Deposits of the Challis 1 x 2 Degree Quadrangle, Idaho: United States Geological Survey Bulletin 1658F, p. 81-95.
- Childs, J. F. 1983. Geology of the Precambrian Belt Supergroup and northern margin of the Idaho batholith, Clearwater County, Idaho: University of California Ph.D. dissertation, Santa Cruz, 491 p.
- Ewing, T. E. 1980. Paleogene tectonic evolution of the Pacific northwest: Journal of Geology, v. 88, p. 609-618.
- Hardyman, R. F. 1981. Twin Peaks caldera of central Idaho. Montana Geological Society Field Conference and Symposium Guidebook, Southwest Montana, p. 317-322.
- Hietanen, A. 1963. Idaho batholith near Pierce and Bungalow, Clearwater County, Idaho: United States Geological Survey Professional Paper 344-D, 42 p.
- . 1969. Distribution of Fe and Mg between garnet, staurolite, and biotite in aluminum-rich schist in various metamorphic zones north of the Idaho batholith: American Journal of Science, v. 267, p. 422-456.
- Hyndman, D. W., and D. A. Foster. 1988. The role of tonalites and mafic dikes in the generation of the Idaho batholith: Journal of Geology, v. 96, p. 31-46.
- Leonard, B. F., and R. F. Marvin. 1982. Temporal evolution of the Thunder mountain caldera and related features, central Idaho, *in* Bonnichsen, B. and Breckenridge, R. M., editors. Cenozoic Geology of Idaho: Idaho Geological Survey Bulletin 26, p. 23-41.
- Lewis, R. S. 1990. Geology, geochemistry and mineral potential of Cretaceous and Tertiary plutons in the eastern part of the Soldier Mountains, Idaho: Oregon State University PhD dissertation, Corvallis, 213 p.
- Lewis, R. S., and T. H. Kiilsgaard. 1991. Eocene plutonic rocks in south central Idaho: Journal of Geophysical Research, v. 96, p. 13295-13311.
- Lewis, R. S., R. F. Burmester, M. D. McFadden, B. A. Eversmeyer, C. A. Wallace, and E. H. Bennett. 1992a. Geologic map of the Upper North Fork of the Clearwater River area, northern Idaho: Idaho Geological Survey Geologic Map series, 1:100,000.
- Lewis, R. S., R. F. Burmester, R. W. Reynolds, E. H. Bennett, P. E. Myers, and R. R. Reid. 1992b. Geologic map of the Lochsa river area, northern Idaho: Idaho Geological Survey Geologic Map series, 1:100,000.
- Marvin, R. F., H. H. Mehnert, C. W. Naeser, and R. E. Zartman. 1989. U. S. Geological Survey radiometric ages—compilation C: Isochron/west, no. 53, p. 3-13.
- Motzer, W. E. 1985. Tertiary epizonal plutonic rocks of the Selway Bitterroot wilderness: University of Idaho Ph.D. dissertation, Moscow, 467 p.
- Nold, J. L. 1968. Petrology of the northeastern border zone of the Idaho batholith (Cretaceous), Idaho and Montana: University of Montana Ph.D. dissertation, Missoula, 159 p.
- Parsons, I. and W. L. Brown. 1984. Feldspars and the thermal history of igneous rocks, *in* Brown, W. L., editor, Feldspars and Feldspathoids, D. Reidel Publishing, Dordrecht, 371 p.
- Ragland, P. C., 1989, Basic Analytical Petrology: Oxford University Press, Oxford, 369 p.
- Reynolds, R. W. 1991. Petrology and geochemistry of the Bungalow pluton and associated hypabyssal dikes, Clearwater County, Idaho: University of Idaho MS thesis, Moscow, 204 p.
- Simpson, S. J. 1985. Structure and petrology of the Rhodes Peak cauldron, Montana and Idaho: University of Montana MS thesis, Missoula, 104 p.
- Zeit, I., F. P. Gilbert, and J. R. Kirby. 1978. Aeromagnetic and gravity maps of Idaho: United States Geological Survey Geophysical Investigation GP-920.

Received 15 February 1995

Accepted for publication 24 September 1995